High frequency diagnostics on the CORONAS-I satellite

A. Kiraga

Space Research Center, ul. Bartycka 18A, 00-716, Warsaw, Poland, kiraga@cbk.waw.pl

Abstract

Quasi simultaneous data on High Frequency (HF) noise, antenna impedance and topside sounder were registered on-board the CORONAS-I satellite which operated in a nearly circular orbit of 500 km altitude and 82.5 deg inclination. Relevant details of the instrument operation are presented. We show the relevance of the equivalent circuit approach for identification of plasma density signatures in the noise and impedance data. Examples of on-board reduction of topside sounder data are presented. Examples of electron-density signatures extracted by on-board processing of impedance data and topside sounder data are shown. The advantages of integrated diagnostics for monitoring the plasma density are pointed out.

1. Introduction

Topside sounders may provide almost instantaneous data on electron-density structures in extended regions of the ionosphere and magnetosphere as well as on plasma dynamics induced by sounding pulses [1]. Large volumes of relevant analog data were transmitted to the ground for subsequent processing. The availability of digital data is a prerequisite for the development of programs for automatic recognition of plasma resonances, echo traces and qualifying plasmagrams [2, 3]. A significant part of the data from the Intercosmos-19 and Cosmos-1809 topside sounders was acquired with on-board data storage facility. The required data reduction was performed with the aid of analog circuits. A fourfold on-board reduction of data volume, at the expense of amplitude resolution, was performed in the Ohzora and Akebono projects [4].

There is a bias toward a 'good voltmeter concept' in the interpretation of i*n situ* wave data. In the 'good voltmeter concept', spectral structures in the raw data $U(f)$ remind one of the spectra of the electromotive force $E(f)$ imposed on antenna. An outcome of this concept is a notion of persistent Upper Hybrid noise (UHR) in the data. Two prominent noise bands, with frequencies following the local plasma frequency f_n but with maxima markedly downshifted from f_n, were permanently present in the passive mode HF spectra on the Intercosmos-19 satellite. They were explained as the resonances in the equivalent circuit composed from the capacitive input impedance of the preamplifiers and inductances of monopoles embedded into the ambient and wake plasma. The frequency f_n was determined from the cut-off frequency f_x of the X mode trace. In subsequent satellite projects (ACTIVE, APEX and CORONAS-I) in order to have an estimation of local plasma frequency independent of noise spectra interpretation, noise and impedance measurements were integrated in the processor-controlled instrument. The equivalent circuit approach to data analysis revealed important signatures of local plasma density in passive mode and impedance data [5]. Equivalent circuits pertinent to noise and impedance measurements are presented in [5]. In the CORONAS-I project a transmitter was integrated with noise and impedance measurements. Brief description of instrument parameters, operation, typical results and their relevance for future projects is presented.

2. Generalities on data acquisition

The Solar Radio Spectrometer (SORS) was the only instrument for low energy diagnostics in the CORONAS-I mission. The spacecraft was launched on 2 March 1994 and operated on nearly circular orbit of ~500km altitude and 82.5deg inclination. The satellite was stabilized with one face pointing to the Sun. Diagnostics of high energy particles and fields had priority in satellite operation modes. Due to technical on-board problems on the satellite, coupled with the low solar activity, scientific data are available for two periods within few months in the slowest telemetry mode only.

SORS consisted of two radiospectrometers in the frequency bands 0,1-30MHz (HF range) and 20-300MHz (VHF range), impedance meter (0.1-10MHz), pulsed transmitter (0.5-16MHz) and internal memory ~50kB which operated under processor control. The transmitter was provided by IZMIRAN. All operational frequencies were set

978-1-4244-6051-9/11/$26.00

digitally and held fixed during the most elemental measurement. In contrast to potentially very high data rate from the SORS instrument, the data volume alloted in telemetry storage was rather meager, namely ~ 380kbyte in standard telemetry (RTS) and ~760kbyte in auxiliary telemetry (SSNI). Depending on the mode, the RTS frames could be sampled with periods of 2.56sec, 0.320sec or 0.80msec during sessions lasting at the most of 13h40min, 1h42min and 25min respectively. A dozen or so of subprograms selectable by commands and RTS telemetry rate were developed to provide dedicated snapshots evenly distributed in any RTS telemetry session and reasonably separated along the satellite orbit. The SSNI telemetry was more flexible but to simplify the SORS program the same snapshots were taken in combined RTS+SSNI operation as in the case of RTS active alone.

3. Relevant instrument details

The SORS employed five Weitzmann booms of 7.5m in length and of ~0.03min diameter. The boom mounted on the shadowed satellite surface and antiparallel to the sun direction was employed as the impedance sensor. The HF receiver and the transmitter were connected to separate, perpendicular to each other dipoles which were mounted in the plane perpendicular to the sun direction. An angle between an impedance sensor and the Earth magnetic field is computed from satellite position and IGRF field. Other relevant angles of antennas are unknown. While activated the transmitter sent pulses of 100micros duration with a period of ~11msec. The HF receiver featured sensitivity of 1microV, bandwidth of 25kHz, time constant of 80micros and logarithmic compression at the output. One spectrum value was set to arithmetical average of 8 output amplitudes sampled at the rate of ~15kHz. The same procedure was applied to estimate presumably background noise just before the transmitter pulse. Collection of such values on pertinent frequency mesh provided *U(f)* spectrum. The ~15kHz sampling rate was also employed after transmitter pulse. The first echo was measured 320micros after pulse end and 99 echoes were stored for further processing. Self impedance measurements were performed in a voltage divider configuration with a voltage (rms amplitude of 100mV) imposed on one of the antenna arms through the fixed resistor. Only the voltage measured in front of a voltage follower is available (a base voltage *V(f)*). Almost all SORS data were registered with subprograms (modes) T44 and T46.

In the mode T44 the single snapshot contains one HF noise spectrum *U(f)*, one base voltage spectrum *V(f)*, and one VHF spectrum which demand 400bytes, 200bytes and 200 bytes respectively. Only one value of *U(f)*, or *V(f)* was provided for every frequency of respective mesh. Equidistant mesh for *V(f)* spectra (range 0.1-10.05MHz, step 50kHz) was swept in 1s. Hereafter the words 'range' and 'step' will be skipped in equidistant mesh description. Four subranges (0.1-2.575MHz, 25kHz), (2.60-10.05MHz, 50kHz), (10.10 – 15.00MHz, 100kHz), (15.15-30MHz , 150kHz) were swept in 1.5s in the case of *U(f)* spectra. The snapshot was repeated with a period of ~40s while RTS and SSNI operated and a period of ~120s while RTS operated alone. The T44 mode has provided principal data for understanding, validating and pursuing of equivalent circuit approach to diagnostics of HF spectra in the near Earth plasma with use of cylindrical antennas.

The mode T46 features substantial on-board data reduction. In single snapshot the sounding sequence on the 150 frequencies in subranges (0.5-4.0MHz, 50kHz), (4.05-7.95MHz, 100kHz), (8.05-15.65MHz, 200kHz) was followed by *V(f)* measurements on the mesh (0.1-10.075MHz, 25kHz) and subsequent sounding sequence on the 500 frequencies in subranges (0.1-5.075MHz, 25kHz), (5.1-10.075MHz, 25kHz) and (10.1-15.05MHz, 50kHz). In the case of the first sounding sequence, for every frequency, the background noise *U(f)* and ordered indexes of 3 larges echoes were put to telemetry. The second sounding sequence was aimed to determine more precisely the frequency index of the 'largest response' in each of 3 frequency subranges. The 'largest response' means the greatest difference between average of echoes indexed from 9 to 24 and respective background noise *U(f)*. In this way total of 500*99 echo amplitudes was reduced to 3 bytes. Reduction of *V(f)* spectrum is explained below.

It is convenient to characterize the equivalent circuit pertinent to noise measurements with a transfer function

$$T(f) = 10\log\{U(f)/E(f)\} \tag{1}$$

As a result of decreasing awareness of adverse influence of real time telemetry on receiver, the filters in preamplifiers featured diminishing steepness what resulted in increasing input resistance R_i in consecutive missions.

An example of transfer functions *T(f)* computed for respective preamplifiers with the Balmain antenna impedance formula are shown in Figure 1a. In Figure 1b numerical simulations of base voltage *V(f)* show extreme patterns, characterized by absolute maximum which is sharp on the upper hybrid frequency f_u for low plasma densities (strongly magnetized pattern) and bell like at the circuit parallel resonance frequency F_R for sufficiently dense plasma (weakly magnetized pattern). To the right of frequency F_R there is local maximum at frequency f_u

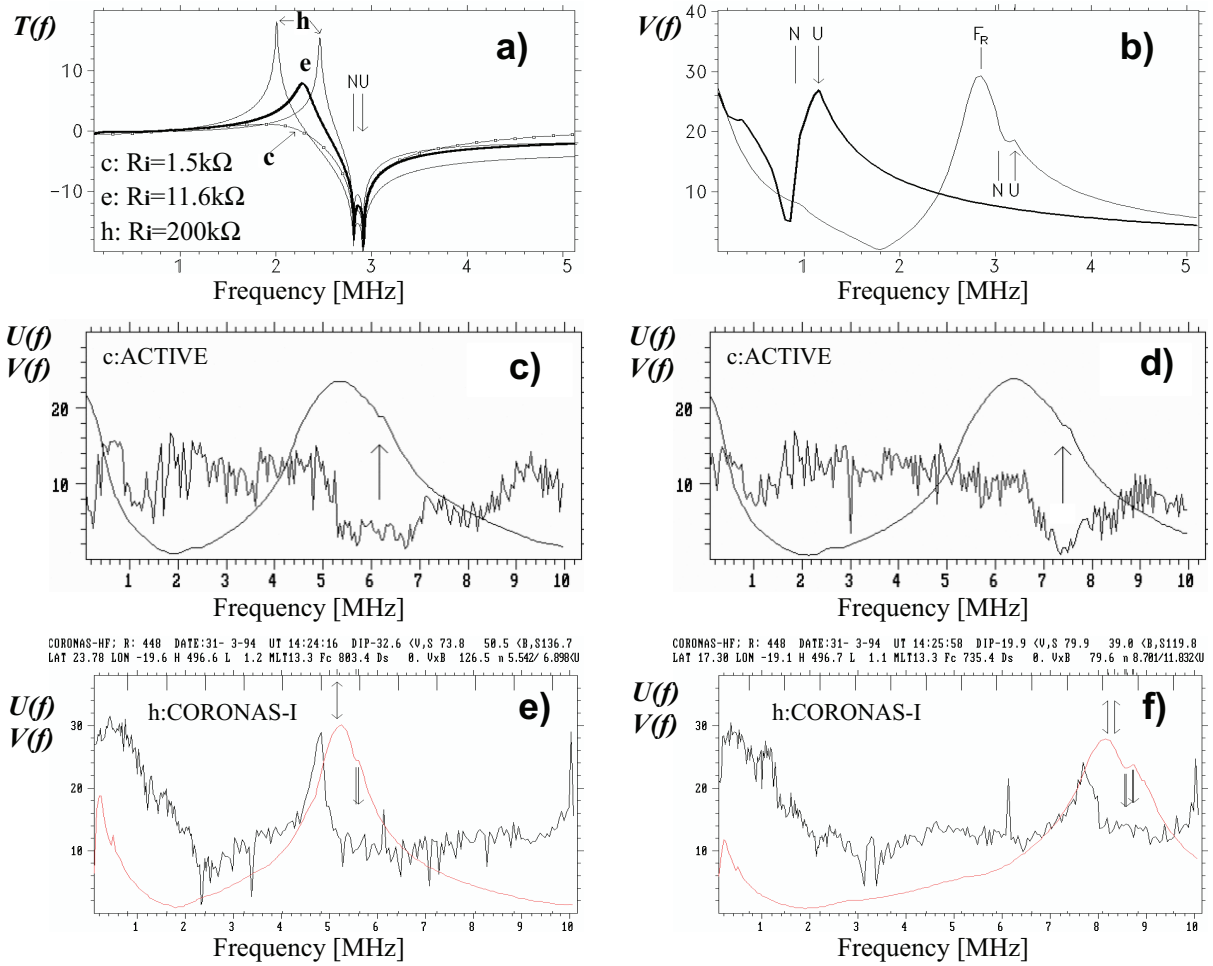

Figure 1. a) Transfer functions pertinent to the ACTIVE (c), APEX (e) and CORONAS-I (h) preamplifiers for gyrofrequency f_c =1MHz and stray capacitance of 30pF. Plasma f_n (| N) and upper hybrid f_u (↑↓U) frequencies are indicated. The highest spike corresponds to an added parallel capacitance of 60pF. Respective input resistances are shown in inset. b) *V(f)* simulations for f_c =0.7MHz, f_n =0.9MHz (bold line) and f_c =1.02MHz, f_n =3.02MHz. c)-f) quasi simultaneous (*U(f)*,*V(f)*) spectra from the ACTIVE and CORONAS-I (T44 mode). *V(f)* shows up as fairly smooth curve and *U(f)* is irregular. Spectra in c) and d) refer to equatorial region at LON~ -168^0, altitude H~800km, and magnetic local time MLT~19h. Respective values are shown above the upper frame in e) and f). In panels c) and d) an arrow points presumable signature of (f_n, f_u) band. In panels e) and f) inner markers attached to upper frame mark gyroharmonics nf_c. Z mode cut off frequency f_z is indicated with ↔ . f_z pointer may be split vertically and separated if two assignments were done. *V(f)* – arb. units. Frequency step of 50kHz pertains to c), d).

providing the direct signature of plasma density. Some subset of weakly magnetized patterns reminding above simulation was found in data from the ACTIVE and APEX satellites. In mode T46 instead of 400 values of *V(f)* only *V(*2MHz*)*, *V(*5MHz*)*, *V(*F_R *)*, F_R, *V(*F_u *)* and F_u were telemetered, where F_u is the frequency of the local maximum to the right of absolute maximum at F_R. The step of 25kHz was employed to increase a chance of F_u capture.

4. Data overview and conclusions

In Figure 1 simulations are confronted with typical data. The most striking is appearance of a narrow banded enhancement in transfer function *T(f)* and noise spectra *U(f)* pertaining to high input resistance preamplifier and absence of analogous structure in the case of low input resistance preamplifier. The *V(f)* data show up weakly magnetized pattern but only in Figure 1f there is a local maximum. Frequency f_u was assigned to slope discontinuity in Figure 1e and to local extrema in Figure 1f as indicated with arrows. In both cases the banded enhancement

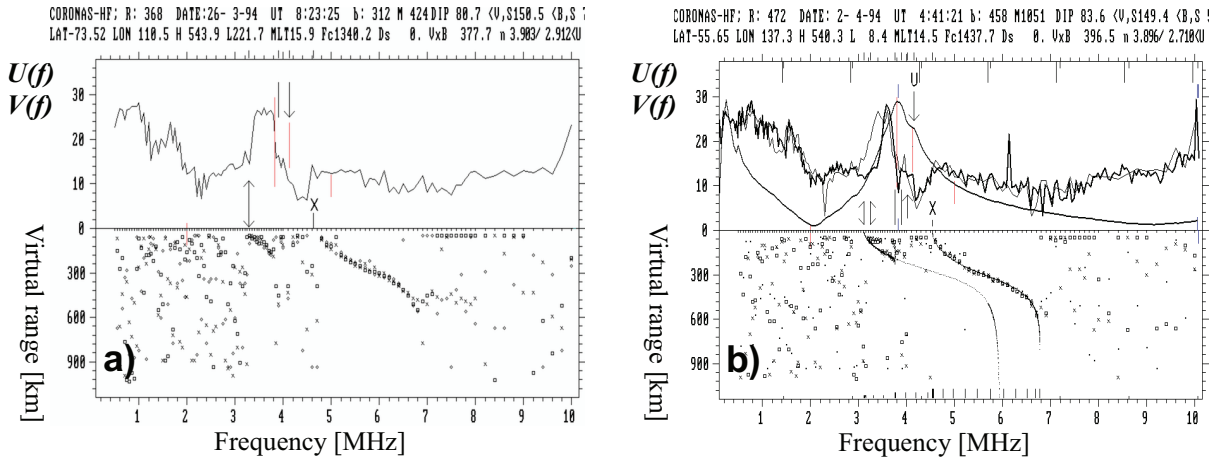

Figure 2. Data from T46 mode. Snapshot data are separated into the echoes section and the *U(f)*+reduced data section. *V(*2MHz*)*, *V(*5MHz*)*, *V(F_R)*, F_R, *V(F_u)* and F_u are in red with upper ends at respective *V(f)*. Frequencies of the largest response are in blue and are discarded in a). b) T46 mode is confronted with (*U(f)*,*V(f)*) pair from T44 mode given with the bold line. Markers of nf_c have different length for different snapshots.

is much broader then the difference f_u - f_n and is downshifted from frequencies F_R and the Z mode cut off f_Z. These relations argue with ambient local upper hybrid noise or electromagnetic Z mode origin. A bandwidth of *V(f)* slope irregularity significantly exceeds f_u - f_n in Figure 1f what is typical for high plasma densities. One of viable mechanisms are Bernstein waves. Features like Z and X mode traces show up only in some subset of echo data in the T46 mode. Impedance data bolster assignment of traces as shown in Figure 2. In Figure 2a frequencies f_Z, f_n, f_X were computed after assignment of f_u to F_u. Computed f_Z, f_X (pointed with x) are in proximity to traces onsets. In Figure 2b one set of frequencies f_Z, f_n, f_u was obtained from f_X (pointed with X) pertinent to fitted trace and the other set was obtained as in Figure 2a. Both sets of cold magneto plasma frequencies compare well and frequency of the largest response is between frequencies f_n. Suitably selected (*U(f)*,*V(f)*) pair from T44 mode separated by several days draw attention to (*U(f)*,*V(f)*) spectra reproducibility, their dependence on the f_n/f_c ratio and better chance of F_u capture with denser frequency mesh. Broadening of banded structure in *U(f)* in T46 mode may be related to enhanced interference from transmitter circuitry and to unquenched plasma reaction to the preceding pulse.

Quasi simultaneous data were registered in favorable experimental configurations set by very different input resistances of noise receivers preamplifiers and simplified technique of impedance measurements. Data analysis driven by equivalent circuit simulations has revealed diversity of local plasma density signatures. Many conflicting past observations may be reconciled. Valuable experience for design of future experiments has been gained.

4. References

1. R. Benson, "Evidence for stimulation of field-aligned electron density irregularities on a short time scale by ionospheric topside sounders," *J. Atmospheric and Solar and Terrestrial Physics*, **59**, 1997, pp. 2281-2293.

2. X. Huang, B. Reinisch, D. Bilitza, and R. Benson, "Electron density profiles of the topside ionosphere," *Annals of Geophysics*, **45**, 2002, pp. 125-130.

3. I. Galkin, B. Reinisch, G. Grinstein, G. Khmyrov, A. Kozlov, X. Huang, and S. Fung, "Automated exploration of the radio plasma imager data," *J. Geophys. Res.*, **109**, 2004, A12210, doi: 10.1029/2004JA010439.

4. H. Oya, A. Morioka, K. Kobayashi, M. Iizima, O. Ono, H. Miyaoka, O. Okada, and T. Obara, "Plasma wave observation and sounder experiments (PWS) using Akebono (EXOS-D) satellite – instrumentation and initial results including discovery of the high altitude equatorial plasma turbulence," *J. Geomag. Geoelectr.*, **42**, 1990, pp. 411-442

5. Kiraga, A. "An investigation of high frequency auroral plasma emissions with a tubular dipole antenna," *Adv. Space Res.* **45**, 2010, doi:10.1016/j.asr.2009.08.028, pp. 553-575.